Spin-valley caloritronics in silicene near room temperature

Xuechao Zhai,[1,*] Wenwen Gao,[2] Xinlong Cai,[2] Ding Fan,[2] Zhihong Yang,[1] and Lan Meng[2]
[1]*Information Physics Research Center, Nanjing University of Posts and Telecommunications, Nanjing 210023, China*
[2]*College of Electronic Science and Engineering, Nanjing University of Posts and Telecommunications, Nanjing 210023, China*
(Received 15 August 2016; revised manuscript received 11 October 2016; published 2 December 2016)

Two-dimensional silicene, with an observable intrinsic spin-orbit coupling, has a great potential to perform fascinating physics and new types of applications in spintronics and valleytronics. By introducing an electromotive force from a temperature difference in ferromagnetic silicene, we discover that a longitudinal spin Seebeck effect can be driven even near room temperature, with spin-up and spin-down currents flowing in opposite directions, originating from the asymmetric electron-hole spin band structures. We further propose a silicene field-effect transistor constructed of two ferromagnetic electrodes and a central dual-gated region, and find that a valley Seebeck effect appears, with currents from two different valleys flowing in opposite directions. The forbidden transport channels are determined by either spin-valley dependent band gaps or spin mismatch. By tuning the electric field in the central region, the transport gaps depending on spin and valley vary correspondingly, and a transition from valley Seebeck effect to spin Seebeck effect is observed. These spin-valley caloritronic results near room temperature are robust against many real perturbations, and thus suggest silicene to be an excellent candidate for future energy-saving technologies and bidirectional information processing in solid-state circuits.

DOI: 10.1103/PhysRevB.94.245405

I. INTRODUCTION

Spin caloritronics, which takes advantage of both spintronics and thermoelectronics, explores the possibility of directly converting heat into electrical power and thus provides a promising way to utilize the dissipating heat or waste energy in modern solid-state devices [1–7]. The most fascinating feature of spin caloritronics is that thermospin currents can be driven by a temperature difference in the absence of external bias voltage [3]. In the past decade, spin caloritronics has attracted much attention, specifically for the continuous experimental progress in spin Seebeck effect, with spin-up and spin-down currents flowing in opposite directions [8–14]. Phenomenally, the longitudinal (transverse) spin Seebeck effect indicates that the current directions are parallel (vertical) to the temperature gradient [15–17]. Physically, spin Seebeck effect generally arises from magnon-driven or phonon-dragged mechanisms in ferromagnetic metals or insulators [18,19]. The latest theoretical studies have proved that zigzag-edged graphene nanoribbons might be good candidates for spin caloritronics [20–23] or valley caloritronics [24], but actually it still costs too much to fabricate such well-edged samples precisely [25–27]. Because spin and valley are difficult to be broken simultaneously due to high symmetries [28–33], bulk graphene and its nanoribbons seem not to be ideal materials to realize the simultaneous control of spin and valley in caloritronics. Conceivably, a huge application prospect will be stimulated if a bulk good-production material could be recognized as an excellent candidate for spin-valley caloritronics.

Silicene, as one of the most popular two-dimensional materials after graphene [34,35], has an observable intrinsic spin-orbit coupling owing to its buckled structure [36]. Benefiting from the spin-orbit coupling, many spin-valley related topological edge states in silicene have been predicted theoretically [36–40], typically valley-polarized quantum anomalous Hall state [39]. Considering that spin and valley in bulk silicene can also be controlled by external fields [41–49], it is reasonable to believe that bulk silicene is feasible to perform spin-valley caloritronics. By introducing an electromotive force from a temperature difference in ferromagnetic silicene, we find that a longitudinal spin Seebeck effect is induced, with spin-up and spin-down currents flowing in opposite directions, originating from the asymmetric electron-hole spin band structures. We further propose a silicene field-effect transistor constructed of two ferromagnetic electrodes and a central dual-gated region, and find that valley Seebeck effect with currents from two different valleys flowing in opposite directions is induced. The forbidden transport channels are determined by either spin-valley dependent band gaps or spin mismatch. By tuning the electric field induced by dual gates, a transition from valley Seebeck effect to spin Seebeck effect is observed because the transport gaps depending on spin and valley vary, obviously. The bidirectional transfer of spin-valley information, driven by temperature here, is markedly distinct from the previously studied unidirectional transfer driven by electric means [41–45], and thus provides an effective and particular proposal for future two-way information processing based on solid-state devices. Meanwhile, these caloritronic results pave the way for applying silicene in future energy-saving technologies.

II. TEMPERATURE-DRIVEN CURRENT

Our focused caloritronic device here is composed of three parts, including a left electrode with high temperature T_L, a central region with length L, and a right electrode with low temperature T_R. The transport from left to right is defined as $+x$ direction. The width of a silicene sample in the y direction is denoted by W. The total transmission modes in this device depends on the energy of incident electrons and can be obtained by $\mathcal{T}^s_\eta(\varepsilon) = \sum_n T^s_\eta(\varepsilon, k_{y,n})$, where $\eta(s)$ represents the valley (spin) index and the discrete wave-vector component satisfies $k_{y,n} = \pi n/(NW)$ with $n = 0, \pm 1, \pm 2, \ldots, \pm N$. In the limit

*zxc@njupt.edu.cn

 ©2016 American Physical Society

of $N \to \infty$ ($W \gg L$), the total transmission modes could be described by the integral $\mathcal{T}_\eta^s(\varepsilon) = (W/\pi)\int_{-\infty}^{\infty} T_\eta^s(\varepsilon,k_y)dk_y$, which can be further expressed as

$$\mathcal{T}_\eta^s(\varepsilon) = N_0\frac{k}{\lambda}\int_0^{\pi/2} T_\eta^s(\varepsilon,\phi)\cos\phi d\phi, \quad (1)$$

where $k = \sqrt{k_x^2+k_y^2}$ with $k_y = k\ \sin\phi$, $N_0 = (2W/\pi)\lambda$ with λ denoting the strength of spinorbit coupling. $T_\eta^s(\varepsilon,\phi)$ describes the angle-dependent transmission for each mode. According to the generalized Laudauer-Büttiker transport approach [20,46–48], the spin-valley dependent current, driven by the temperature difference $T_{LR} = T_L - T_R$, reads

$$I_\eta^s(T_L,T_R) = \frac{e}{h}\int_{-\infty}^{+\infty}\mathcal{T}_\eta^s(\varepsilon)[f_L(\varepsilon,T_L) - f_R(\varepsilon,T_R)]d\varepsilon, \quad (2)$$

where $f_{L(R)}$ denotes the Fermi-Dirac distribution function, $f_{L(R)}(\varepsilon,T_{L(R)}) = 1/[\exp(\varepsilon-\varepsilon_F)/k_BT_{L(R)}+1]$. The temperature in minigap silicene plays the role of exciting thermoelectrons [20–24], different from the mechanisms of magnon excitation in ferromagnetic insulators [18]. From the part of the Fermi-distribution difference $f_L - f_R$ in I_η^s, it is understood that electrons with energy higher than the Fermi energy flow from the left high-temperature electrode to the right low-temperature electrode ($f_L - f_R > 0$), resulting in electron current $(I_e)_\eta^s < 0$. Conversely, electrons with energy lower than the Fermi energy flow in the opposite direction ($f_L - f_R < 0$), resulting in hole current $(I_h)_\eta^s > 0$. If the transmission $\mathcal{T}_\eta^s$ is symmetric about the Fermi energy, the electron current and the hole current will cancel out each other, leading to a zero net spin-valley dependent current $I_\eta^s = (I_e)_\eta^s + (I_h)_\eta^s = 0$. This means, no electron-hole asymmetry, no current.

It has been previously proved that, for a pristine silicene sample without external fields, the low-energy effective Hamiltonian can be written as $H_0 = \hbar\upsilon_F(\eta k_x\tau_x + k_y\tau_y) + \eta\lambda\tau_z\sigma_z$, where $\eta = +(-)$ stands for valley K (K'). The first term represents the massless Dirac fermion, where $\upsilon_F \simeq 5.5\times 10^5$ m/s describes the Fermi velocity [36], τ_i ($i = x,y$) denotes the sublattice pseudospin Pauli matrix, σ_z indicates the spin Pauli matrix, and k_i ($i = x,y$) denotes the wave-vector component. The second term denotes the intrinsic spin-orbit coupling with $\lambda = 3.9$ meV [40–43]. It is reasonable to ignore the Rashba-type tiny perturbations here in studying the band structures and transport properties, as proved by previous first-principles calculations [36,37,41]. For brief notation, below we set $\hbar = 1$, $\upsilon_F = 1$. Then the Hamiltonian reads $H_0 = (\eta k_x\tau_x + k_y\tau_y) + \eta\lambda\tau_z\sigma_z$. Because both spin and valley are degenerate in pristine silicene, no spin-polarized and valley-polarized current can be driven only by a temperature difference.

Under the influence of a uniform ferromagnetic field induced by substrate on a silicene sample [46–49], the system Hamiltonian is given by

$$H = H_0 + M\sigma_z, \quad (3)$$

where M indicates the strength of the ferromagnetic field. The energy bands are solved as

$$\varepsilon(k) = sM + \alpha\sqrt{k^2+\lambda^2}, \quad (4)$$

where the spin index $s = +(-)$ represents spin up (down), and the band index $\alpha = +(-)$ denotes the conduction (valence) bands. Then the energies at valleys K and K' ($k = 0$), read $\epsilon_\alpha^{s,\eta} = sM + \alpha\lambda$. The spin-valley dependent energy gap at K or K' is $(\varepsilon_g)_\eta^s = \epsilon_+^{s,\eta} - \epsilon_-^{s,\eta} = 2\lambda$. The role of the ferromagnetic field here is to move up (down) the spin up (down) subbands. Because M is uniform in both the electrodes and the central dual-gated region, all the transmissions are complete [i.e., $T_\eta^s(\varepsilon,\phi) = 1$, independent of incident angle ϕ] beyond the band-gap region $[\epsilon_-^{s,\eta},\epsilon_+^{s,\eta}]$ where $T_\eta^s(\varepsilon,\phi) = 0$. According to Eq. (1), the spin-valley dependent transmission as a function of energy is obtained as

$$\mathcal{T}_\eta^s(\varepsilon) = \begin{cases} 0, \text{ if } \varepsilon \in [\epsilon_-^{s,\eta},\epsilon_+^{s,\eta}] \\ N_0k/\lambda, \text{ else.} \end{cases} \quad (5)$$

Here, $k = \sqrt{(\varepsilon - sM)^2 - \lambda^2}$. Then the spin-valley dependent current is calculated from Eq. (2) as

$$I_\eta^s = -I_0\int_D \frac{k}{\lambda}[f_L(\varepsilon,T_L) - f_R(\varepsilon,T_R)]d\varepsilon, \quad (6)$$

where the integral interval D covers the region $(-\infty,\epsilon_-^{s,\eta}]$ contributed to $(I_h)_\eta^s$ and the region $[\epsilon_+^{s,\eta},\infty)$ contributed to $(I_e)_\eta^s$, and the constant $I_0 = -N_0e/h > 0$ is used here as the reduced value of I_η^s in plotting figures.

In Fig. 1, we show the reduced current I_η^s/I_0 as a function of the temperature T_L at $T_{LR} = 20$ K, $M = \lambda$, and $\ell E_z = \varepsilon_F = 0$ (E_z is the strength of interlayer electric field). The ferromagnetic-silicene device is shown by the bottom-left inset, and the energy bands denoted by spin and valley indexes are given in the bottom-right inset. The ferromagnetic field here only breaks the spin degeneracy of bands but does not break the valley degeneracy. Our calculations indicate that

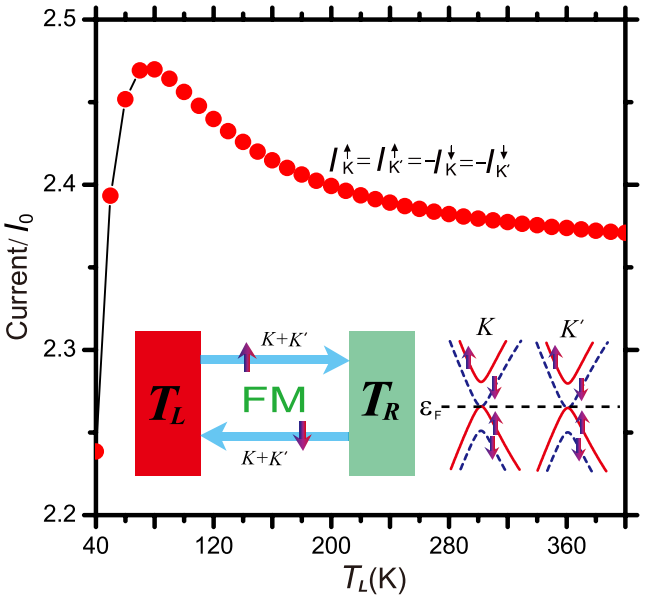

FIG. 1. Reduced current I_η^s/I_0 vs temperature T_L at $T_{LR} = 20$ K, $M = \lambda$, and $\ell E_z = \varepsilon_F = 0$. The corresponding device is shown by the bottom-left inset and the energy bands of silicene under a ferromagnetic (FM) field are given by the bottom-right inset. $T_{L(R)}$ indicates the temperature of the left (right) thermoelectrode, and the arrows point to the current directions.

the spin-valley dependent current satisfies $I_K^{\uparrow} = I_{K'}^{\uparrow} = -I_K^{\downarrow} = -I_{K'}^{\downarrow}$, which means spin-up and spin-down currents (independent of valley) flowing in opposite directions, corresponding to the longitudinal spin Seebeck effect [16]. This effect arises from the electron-hole asymmetry of spin bands. The asymmetry of the spin-up transport gap $[0,2\lambda]$ about the Fermi energy $\varepsilon_F = 0$ leads to $|(I_e)_\eta^{\uparrow}| < (I_h)_\eta^{\uparrow}$, while that of the spin-down gap $[-2\lambda,0]$ leads to $|(I_e)_\eta^{\downarrow}| > (I_h)_\eta^{\downarrow}$. Hence, $I_\eta^{\uparrow}$ is dominated by holes ($I_\eta^{\uparrow} > 0$) from the valence bands, while $I_\eta^{\downarrow}$ is dominated by electrons ($I_\eta^{\downarrow} < 0$) from the conduction bands. Specifically, $|I_\eta^s|$ at a given T_L is the same for any spin valley, attributed to the antispin electron-hole symmetries of energy bands. Therefore the current driven by T_{LR} here is completely spin polarized but valley unpolarized although the net charge current $I = \sum_{s,\eta} I_\eta^s$ is always zero. Note that $|I_\eta^s|$ for any spin valley first increases and then decreases as T_L increases. The reason behind this is the competition effect between the increasing transport modes induced by larger temperature broadening and the decreasing driven force described by T_{LR}/T_L. Under $T_{LR} \ll T_L \simeq T_R$, I_η^s in Eq. (6) could be expressed as

$$I_\eta^s \simeq I_0 \frac{T_{LR}}{T_L} \int_D \frac{\varepsilon}{\lambda} \sqrt{(\varepsilon - sM)^2 - \lambda^2}\, d\left(\frac{1}{e^{\varepsilon/(k_B T_L)} + 1}\right). \quad (7)$$

As T_L continues to increase, $|I_\eta^s|$ tends to be a stable value, which is about $2.37 I_0$ in Fig. 1.

III. CALORITRONIC FIELD-EFFECT TRANSISTOR

Since we have proved that silicene with ferromagnetic field can support a spin Seebeck effect under the driving force of temperature difference, we further ask such questions, "Does valley Seebeck effect exist as a counterpart of spin Seebeck effect? If yes, how can valley and spin in Seebeck effects be modulated and switched conveniently?" To answer these questions, we now propose a silicene-based caloritronic field-effect transistor, which includes two thermoelectrodes (left source and right drain) with ferromagnetic field and a central dual-gated region with an interlayer electric field E_z, as sketched in Fig. 2(a). The more fundamental transport in a single junction is included in the Supplemental Material [50]. Compared with the simple case in Eq. (3), the system Hamiltonian here should be expressed as

$$\mathcal{H} = H_0 + M\sigma_z Q(x) - \ell E_z \tau_z Q'(x), \quad (8)$$

where $Q(x) = \Theta(-x) + \Theta(x - L)$, $Q'(x) = \Theta(x) - \Theta(x - L)$ with $\Theta(x)$ the Heaviside function, and ℓE_z with $\ell = 2.86$ Å indicates the interlayer potential difference induced by E_z. The energy bands in Eq. (4) are replaced by

$$\varepsilon(k) = sMQ(x) + \alpha\sqrt{k^2 + [\ell E_z Q'(x) - s\eta\lambda]^2}, \quad (9)$$

The energies at valleys K, K' ($k = 0$) read $\epsilon_\alpha^{s,\eta} = sMQ(x) + \alpha|\ell E_z Q'(x) - s\eta\lambda|$.

Note that the translational invariance of the system described by Eqs. (8) and (9) is broken, and thus plane-wave solutions with the same wave vector are no longer the eigenstates. At a given energy ε, we obtain the wave-vector modulus in the electrodes and the central dual-gated region, respectively, as $k = \sqrt{(\varepsilon - sM)^2 - \lambda^2}$, $q = \sqrt{\varepsilon^2 - (\lambda_V - s\eta\lambda)^2}$. According to the requirement of wave-function continuity in quantum mechanics, we derive the transmission amplitude by matching

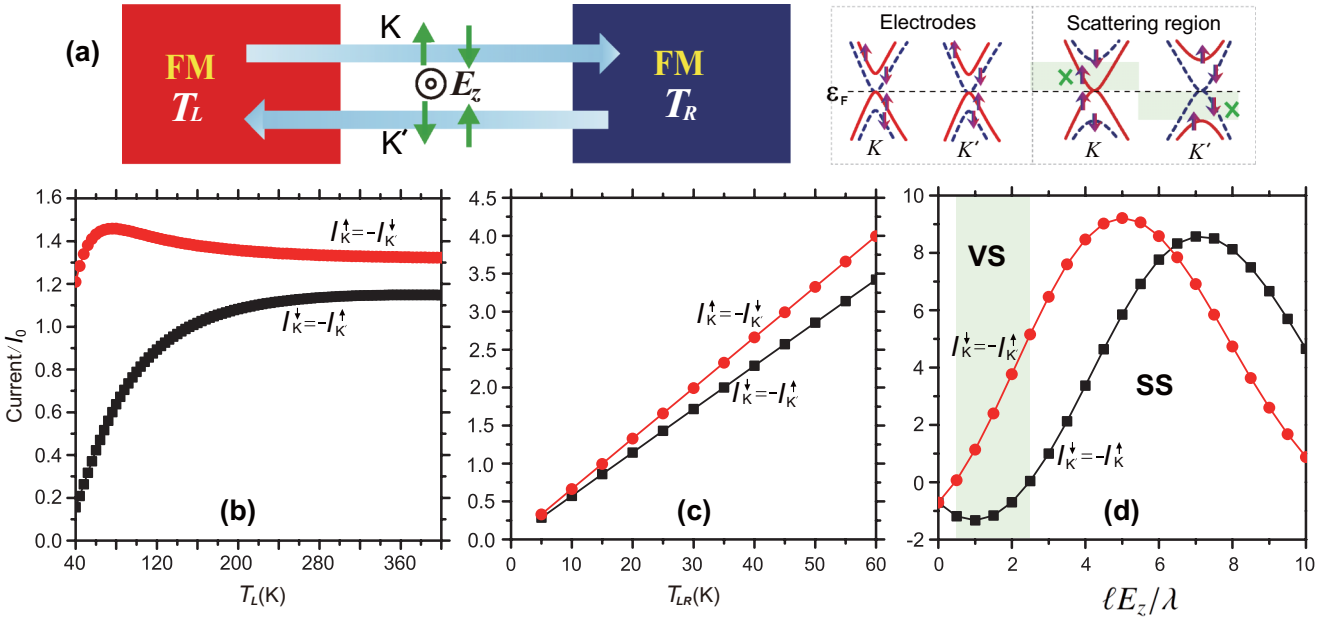

FIG. 2. (a) Schematic of silicene-based caloritronic field-effect transistor. A ferromagetic field is applied in the left and right thermoelectrodes, and an interlayer electric field is applied in the central region. A phenomenon of valley Seebeck effect is sketched, corresponding to the energy subbands on the right side, where the shaded areas indicate the transport gaps of spin-up (down) from valley K (K') due to spin band gaps and spin mismatch. (b) Reduced current I_η^s/I_0 vs temperature T_L at $T_{LR} = 20$ K, $\ell E_z = \lambda$, and $\varepsilon_F = 0$. (c) Reduced current I_η^s/I_0 vs temperature T_{LR} at $T_L = 320$ K, $\ell E_z = \lambda$. (d) Reduced current I_η^s/I_0 vs electric field ℓE_z at $T_L = 300$ K, $T_{LR} = 20$ K. VS and SS represent valley Seebeck effect and spin Seebeck effect, respectively.

the wave functions at the interfaces $x = 0, L$ as

$$t_\eta^s(\phi) = \frac{2\chi\chi' e^{i\kappa L}\cos\phi[\sin(q_x L)e^{-i\eta\theta} + i\ \cos\theta']}{F[\chi\ \sin(q_x L)e^{-i\eta\phi} + i\chi'\cos\theta'] + iF'\chi'\cos\theta}, \tag{10}$$

where $\chi = (\varepsilon + s\eta\lambda - sM)/k$, $\chi' = (\varepsilon - \lambda_V + s\eta\lambda)/q$, $\kappa = q\ \cos\theta - k\ \cos\phi$, and $\theta = \pi - \arcsin(k\sin\phi/q)$. The angular-dependent functions F, F' are obtained as $F = \chi e^{i\eta\phi} + \chi' e^{-i\eta\theta}, F' = \chi e^{-i\phi'} - \chi' e^{-i\theta'}$, where $\phi' = \eta\phi - qL\cos\theta$ and $\theta' = \eta\theta - qL\cos\theta$. The transmission coefficient in Eq. (1) is then given by $T_\eta^s(\varepsilon,\phi) = |t_\eta^s(\phi)|^2$. It should be noted that the parameter $L = 50$ nm is used to carry out the following calculations and plot figures. The energy bands for the electrodes and the central region, at $\varepsilon_F = \ell E_z = \lambda$, are shown on the right side of Fig. 2(a). There are two factors that induce transport gaps: (i) spin-valley dependent band gaps for both the electrodes and the central dual-gated region, and (ii) spin mismatch between the electrodes and the central region. By analyzing, the transport gap for spin-up (down) electrons from valley K (K') is indicated by the shaded area $[0,2\lambda]$ ($[-2\lambda,0]$) in the central region. Likewise, one can obtain the transport gap for spin-down (up) electrons from valley K (K') as $[-2\lambda,2\lambda]$.

In Fig. 2(b), we show the reduced current I_η^s/I_0 as a function of the temperature T_L at $T_{LR} = 20$ K, $\ell E_z = \lambda$, and $\varepsilon_F = 0$. Compared with Fig. 1, the band-matching degree between the electrodes and the central dual-gated region is reduced and thus $|I_\eta^s|$ for any spin valley decreases under the same temperature situation. Judged from the transport gap $[0,2\lambda]$ ($[-2\lambda,0]$) in Fig. 2(a) for spin-up (down) from valley K (K'), we conclude that the currents contributed by $(I_e)_\eta^s$ and $(I_h)_\eta^s$ cannot cancel out each other due to the asymmetry of the transport gap about the Fermi energy $\varepsilon_F = 0$. It is the holes (electrons) that contribute most to the nonzero current $I_K^\uparrow$ ($I_{K'}^\downarrow$). For spin-down (up) electrons from valley K (K'), the transport gap $[-2\lambda,2\lambda]$ is symmetric about the Fermi energy, while such electron-hole symmetry cannot drive a nonzero current. Actually, it is the electron-hole asymmetry of spin bands in the ferromagnetic electrodes that should be responsible for the nonzero $I_K^\downarrow$ and $I_{K'}^\uparrow$. Considering that the matching degree between the electrodes and the central region for spin-down electrons in the valence band is better than that in the conduction band due to the smaller wave-vector difference, we have $|(I_e)_K^\downarrow| < (I_h)_K^\downarrow$, which indicates $I_K^\downarrow$ is dominated by holes ($I_K^\downarrow > 0$). Likewise, it can be understood that $I_{K'}^\uparrow$ is dominated by electrons ($I_{K'}^\uparrow < 0$). Thus it is no surprise that the phenomenon of valley Seebeck effect happens in Fig. 2(a), as a counterpart of the spin Seebeck effect in Fig. 1. As T_L continues to increase, the absolute values of I_η^s gradually tend to stabilize, as has been demonstrated in Fig. 1. Additionally, below 20 K (consider a smaller T_{LR}), $I_K^\downarrow$ and $I_{K'}^\uparrow$ are too small to be ignored compared with $I_K^\uparrow$ and $I_{K'}^\downarrow$, and thus the system could support valley Seebeck effect and spin Seebeck effect simultaneously [50].

Figure 2(c) plots the reduced current I_η^s/I_0 vs the temperature difference T_{LR} at $T_L = 320$ K, $\ell E_z = \lambda$, and $\varepsilon_F = 0$. The relations $I_K^\uparrow = -I_{K'}^\downarrow$ and $I_K^\downarrow = -I_{K'}^\uparrow$ always hold because the band symmetry is not destroyed by T_{LR}. As T_{LR} increases, the electromotive force is enhanced and thus $|I_\eta^s|$ for any spin valley increases. The curves of I_η^s vs T_{LR} here tell us a simple rule that the temperature difference could enhance the thermospin current almost linearly, because the relation $I_\eta^s \propto T_{LR}$ in Eq. (7) still holds. In addition, the absolute values of $I_K^\uparrow$ and $I_{K'}^\downarrow$ increase more rapidly than that of $I_K^\downarrow$ and $I_{K'}^\uparrow$ as T_{LR} increases. This results from a fact that the energy gap $(\varepsilon_g)_K^\uparrow = (\varepsilon_g)_{K'}^\downarrow = 0$ is much smaller than the energy gap $(\varepsilon_g)_K^\downarrow = (\varepsilon_g)_{K'}^\uparrow = 4\lambda$. At a given T_{LR}, the smaller the spin-valley dependent gap is, the larger the corresponding current is. Under the condition of $T_{LR} \to 0$, the driving force tends to zero and thus all the currents I_η^s tend to zero, as expected.

Figure 2(d) plots the reduced current I_η^s/I_0 vs the electric field ℓE_z at $T_L = 300$ K, $T_{LR} = 20$ K, and $\varepsilon_F = 0$. As ℓE_z increases, the transport gaps $[\epsilon_-^{s,\eta}, \epsilon_+^{s,\eta}]$ for spin-valley currents vary correspondingly, with $\epsilon_\pm^{s,\eta} = \pm|\ell E_z - s\eta\lambda|$. It is found that the valley Seebeck effect [see Fig. 2(a)] is always detectable in the shaded region $0.5\lambda < \ell E_z < 2.5\lambda$, beyond which the spin Seebeck effect is observed. The transition point between valley Seebeck effect and spin Seebeck effect happens at $\ell E_z \simeq 0.5\lambda$ or 2.5λ when it satisfies $(I_\eta^s)_{s\eta=-1} = 0$, which is an inevitable consequence of electron-hole current cancellation as the transport gaps depending on spin and valley vary. The difference between the left and right unshaded spin-Seebeck regions is that all the directions of I_η^s are reversed. Specifically at $\ell E_z = 0$, all the spin-valley dependent currents have the same absolute value due to the spin and valley degeneracies of bands. As ℓE_z increases, the spin-valley dependent band gap $(\varepsilon_g)_K^\uparrow = (\varepsilon_g)_{K'}^\downarrow = 2|\ell E_z - \lambda|$ first decreases and then increases while the gap $(\varepsilon_g)_K^\downarrow = (\varepsilon_g)_{K'}^\uparrow = 2|\ell E_z + \lambda|$ increases monotonously, and thus $(I_\eta^s)_{s\eta=-1}$ and $(I_\eta^s)_{s\eta=1}$ change differently. As ℓE_z continues to increase, the band gaps $(\varepsilon_g)_\eta^s$ in the central dual-gated region become larger and all the spin-valley dependent currents I_η^s tend to zero because the energy broadening induced by temperature cannot go across the transport gap.

Since we have evaluated the thermal spin-valley transport in the ballistic regime by using Landauer-Büttiker formulism, a question about "inelastic scattering" at the higher temperatures naturally arises. As temperature increases, electron-phonon interactions are naturally enhanced because more phonon modes are excited, and thus the electron mobility decreases. There are two possible scattering types: intravalley scattering and intervalley scattering. For intravalley scattering, the increasing of temperature cannot mix the states with different spin (valley) indexes due to the absence of a spin-flip (valley-transfer) mechanism, and nevertheless only reduces the magnitude of I_η^s in Figs. 1 and 2. This means, the qualitative conclusions obtained in the ballistic regime are still valid. For intervalley scattering, the latest first-principles calculations have shown that there exists a critical temperature about 300 K, above which only the electrons with energy more than 30 meV could feel this scattering due to the stronger electron-phonon coupling [51]. Consequently, it is reasonable to believe that our obtained results in silicene are detectable even near room temperature.

Finally, it is necessary to discuss the robustness of silicene-based spin-valley related Seebeck effects on some real complex experimental conditions. Firstly, if a silicene sample

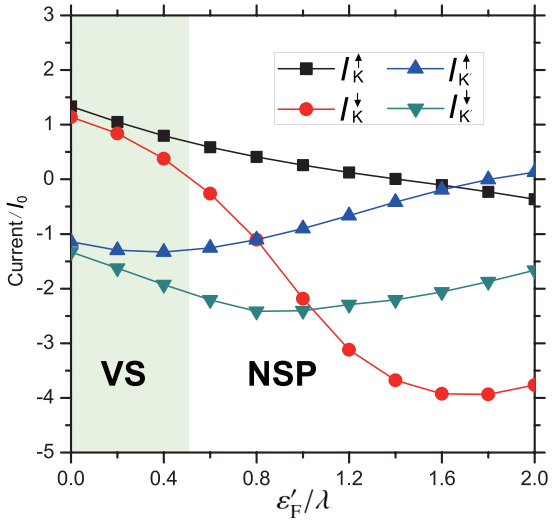

FIG. 3. Reduced current I^s_η/I_0 vs the Fermi energy ε'_F in the central dual-gated region, when the Fermi energy in the two electrodes equals zero. The other parameters are chosen as $M = \ell E_z = \lambda$, $T_L = 300$ K, and $T_{LR} = 20$ K. NSP denotes the normal spin-polarized current.

is undoped ($\varepsilon_F = 0$) in the electrodes but doped ($\varepsilon'_F \neq 0$) in the central dual-gated region, our results in Fig. 3 reveal that valley Seebeck effect is robust at $\varepsilon'_F < 0.5\lambda \simeq 2$ meV. Beyond this region, a normal spin-polarized current can still be detected. We also verify that valley Seebeck effect is also robust under $\varepsilon_F < 0.4\lambda \simeq 1.6$ meV when the silicene sample is uniformly doped ($\varepsilon_F \neq 0$) for both the electrodes and the central dual-gated region [50]. Likewise, one can further prove that the spin Seebeck effect in Fig. 2(d) is robust under a small perturbation of Fermi energy. Secondly, additional results about the influence of ferromagnetic field M and channel length L on Seebeck effects are also included in the Supplemental Material [50]. These further calculations indicate that the spin and valley Seebeck phenomena found here are robust at $M \leqslant \lambda \simeq 4$ meV, and can appear alternately by increasing channel length L. The exchange field M, on the order of meV, can be fully achieved in silicene by using an appropriate ferromagnetic insulating substrate (for instance, EuS) without inducing external Rashba-type interactions, according to the latest experimental report on graphene [52] where such strength of M (depending critically on the sample quality) is realized. Certainly, it is still an open question when one considers some types of magnetic substrates which induce the coexistence of the larger Rashba-type interactions and the field M.Thirdly, a real sample of silicene also inevitably contains structural imperfections, such as bits of vacancies [23], which induce variations of supercell bands. Our caloritronic conclusions are robust when the defect ratio could not exceed about 8%, beyond which these effects are broken by defect states, which lie inside the transport gaps [53]. Fourthly, the influence of the Aharonov-Casher phase associated with the E_z field can be ignored here for two reasons: one is that the Aharonov-Casher phase generally works when an electron propagates in a ring structure [54,55]; the other is that the Aharonov-Casher phase in silicene arises from the Rashba-type interactions [55], which are negligible in studying the transport properties even under external fields [41–43]. Fifthly, considering the negligible influence of weak Rashba-type interactions on the transport properties, it is reasonable to further conclude that the ballistic caloritronic results obtained here are basically robust against the spin-dephasing process [56,57] induced by the momentum scattering due to Rashba-type interactions. Actually, our main conclusions are also tolerant against weak spin-flip scattering induced by local magnetic scatters, but become invalid when the magnetic scattering is strong enough to break the dominated band-selection rule in Figs. 1 and 2. Moreover, the theoretical formalism in this study is also suitable for germanene with stronger intrinsic spin-orbit coupling $\lambda_{so} = 43$ meV [40], which exceeds the energy broadening driven by room temperature. Thus the germanene-based device could also perform spin-valley caloritronics, and the coexistence phenomenon of spin and valley Seebeck effects may be detected even near room temperature.

IV. CONCLUSION

To conclude, by introducing an electromotive force from a temperature difference in a ferromagnetic silicene, we have discovered that a longitudinal spin Seebeck effect can be driven even near room temperature, with spin-up and spin-down currents flowing in opposite directions, originating from the asymmetric electron-hole spin bands. We have further proposed a silicene field-effect transistor constructed of two ferromagnetic electrodes and a central dual-gated region, and found that a valley Seebeck effect appears, with currents from two different valleys flowing in opposite directions. The transport gaps are determined by either spin-valley dependent band gaps or spin mismatch. By tuning the electric field in the central dual-gated region, the symmetric matching condition between electron-hole bands varies significantly, and a transition from valley Seebeck effect to spin Seebeck effect has been observed. Therefore, “temperature” may provide a distinctive, efficient and convenient method to detect and control the spin and valley degrees of freedom. Although much effort has been made previously in exploring the spin-valley dependent phenomena in silicene and its derivatives, the temperature-driven counterpropagating transport associated with Seebeck effects, which supports valley-spin selective net current in each direction, is unique, specifically for the electrically controlled switch between spin Seebeck effect and valley Seebeck effect. Our results suggest silicene to be an outstanding candidate for future energy-saving technologies in heat-treatment solid-state devices as well as future information processing in spin-valley logic circuits.

ACKNOWLEDGMENTS

We thank Professor G. Jin for the helpful discussion. This work was supported by the National Natural Science Foundation of China (Grants No. 11504179 and No. 11504180), the Natural Science Foundation of Jiangsu Province (Grant No. BK20150830), the Universities Natural Science Research Project of Jiangsu Province (Grant No. 15KJB140005), NUPTSF (Grant No. NY214193), SKPBR (No. 2015CB921202), and NUPT-STITP (Grant No. XYB2016049).

[1] J.-C. Le Breton, S. Sharma, H. Saito, S. Yuasa, and R. Jansen, Thermal spin current from a ferromagnet to silicon by Seebeck spin tunneling, Nature (London) **475**, 82 (2011).

[2] R. Jansen, Silicon spintronics, Nat. Mater. **11**, 400 (2012).

[3] G. E. W. Bauer, E. Saitoh, and B. J. van Wees, Spin caloritronics, Nat. Mater. **11**, 391 (2012).

[4] J. Flipse, F. L. Bakker, A. Slachter, F. K. Dejene, and B. J. van Wees, Direct observation of the spin-dependent Peltier effect, Nat. Nanotechnol. **7**, 166 (2012).

[5] G. Fiori, F. Bonaccorso, G. Iannaccone, T. Palacios, D. Neumaier, A. Seabaugh, S. K. Banerjee, and L. Colombo, Electronics based on two-dimensional materials, Nat. Nanotechnol. **9**, 768 (2014).

[6] J. Sinova, S. O. Valenzuela, J. Wunderlich, C. H. Back, and T. Jungwirth, Spin Hall effects, Rev. Mod. Phys. **87**, 1213 (2015).

[7] A. Hoffmann and S. D. Bader, Opportunities at the Frontiers of Spintronics, Phys. Rev. Appl. **4**, 047001 (2015).

[8] K. Uchida, S. Takahashi, K. Harii, J. Ieda, W. Koshibae, K. Ando, S. Maekawa, and E. Saitoh, Observation of the spin Seebeck effect, Nature (London) **455**, 778 (2008).

[9] K. Uchida, J. Xiao, H. Adachi, J. Ohe, S. Takahashi, J. Ieda, T. Ota, Y. Kajiwara, H. Umezawa, H. Kawai, G. E. W Bauer, S. Maekawa, and E. Saitoh, Spin Seebeck insulator, Nat. Mater. **9**, 894 (2010).

[10] C. M. Jaworski, J. Yang, S. Mack, D. D. Awschalom, J. P. Heremans, and R. C. Myers, Observation of the spin-Seebeck effect in a ferromagnetic semiconductor, Nat. Mater. **9**, 898 (2010).

[11] C. M. Jaworski, R. C. Myers, E. Johnston-Halperin, and J. P. Heremans, Giant spin Seebeck effect in a non-magnetic material, Nature (London) **487**, 210 (2012).

[12] D. Qu, S. Y. Huang, J. Hu, R. Wu, and C. L. Chien, Intrinsic Spin Seebeck Effect in Au/YIG, Phys. Rev. Lett. **110**, 067206 (2013).

[13] S. Borlenghi, W. Wang, H. Fangohr, L. Bergqvist, and A. Delin, Designing a Spin-Seebeck Diode, Phys. Rev. Lett. **112**, 047203 (2014).

[14] S. M. Wu, W. Zhang, A. KC, P. Borisov, J. E. Pearson, J. S. Jiang, D. Lederman, A. Hoffmann, and A. Bhattacharya, Antiferromagnetic Spin Seebeck Effect, Phys. Rev. Lett. **116**, 097204 (2016).

[15] Z. Jiang, C.-Z. Chang, M. R. Masir, C. Tang, Y. Xu, J. S. Moodera, A. H. MacDonald, and J. Shi, Enhanced spin Seebeck effect signal due to spin-momentum locked topological surface states, Nat. Commun. **7**, 11458 (2016).

[16] T. Kikkawa, K. Uchida, Y. Shiomi, Z. Qiu, D. Hou, D. Tian, H. Nakayama, X.-F. Jin, and E. Saitoh, Longitudinal Spin Seebeck Effect Free from the Proximity Nernst Effect, Phys. Rev. Lett. **110**, 067207 (2013).

[17] D. Meier, D. Reinhardt, M. van Straaten, C. Klewe, M. Althammer, M. Schreier, S. T. B. Geonnenwein, A. Gupta, M. Schmid, C. H. Back, J.-M. Schmalhorst, T. Kuschel, and G. Reiss, Longitudinal spin Seebeck effect contribution in transverse spin Seebeck effect experiments in Pt/YIG and Pt/NFO, Nat. Commun. **6**, 8211 (2015).

[18] H. Adachi, K.-I. Uchida, E. Saitoh, and S. Maekawa, Theory of the spin Seebeck effect, Rep. Prog. Phys. **76**, 036501 (2013).

[19] S. M. Rezender, R. L. Rodríguez-Suárez, R. O. Cunha, A. R. Rodrigues, F. L. A. Machado, G. A. Fonseca Guerra, J. C. Lopez Ortiz, and A. Azevedo, Magnon spin-current theory for the longitudinal spin-Seebeck effect, Phys. Rev. B **89**, 014416 (2014).

[20] M. Zeng, Y. Feng, and G. Liang, Graphene-based spin caloritronics, Nano Lett. **11**, 1369 (2011).

[21] X. Chen, Y. Liu, B. L. Gu, W. Duan, and F. Liu, Giant room-temperature spin caloritronics in spin-semiconducting graphene nanoribbons, Phys. Rev. B **90**, 121403(R) (2014).

[22] X. F. Yang, Y. S. Liu, J. F. Feng, and X. F. Wang, Thermoelectric and thermospin transport in a ballistic junction of graphene, AIP Adv. **4**, 087116 (2014).

[23] M. Inglot, V. K. Dugaev, and J. Barnaś, Thermoelectric and thermospin transport in a ballistic junction of graphene, Phys. Rev. B **92**, 085418 (2015).

[24] X. Chen, L. Zhang, and H. Guo, Valley caloritronics and its realization by graphene nanoribbons, Phys. Rev. B **92**, 155427 (2015).

[25] X. Li, X. Wang, L. Zhang, S. Lee, and H. Dai, Chemically derived, ultrasmooth graphene nanoribbon semiconductors, Science **319**, 1229 (2008).

[26] P. Ruffieux, S. Wang, B. Yang, C. Sánchez-Sánchez, J. Liu, T. Dienel, L. Talirz, P. Shinde, C. A. Pignedoli, D. Passerone, T. Dumslaff, X. Feng, K. Müllen, and R. Fasel, On-surface synthesis of graphene nanoribbons with zigzag edge topology, Nature (London) **531**, 489 (2016).

[27] A. Narita, X. Feng, Y. Hernandez, S. A. Jensen, M. Bonn, H. Yang, I. A. Verzhbitskiy, C. Casiraghi, M. R. Hansen, A. H. R. Koch, G. Fytas, O. Ivasenko, B. Li, K. S. Mali, T. Balandina, S. Mahesh, S. De Feyter, and K. Müllen, Synthesis of structurally well-defined and liquid-phase-processable graphene nanoribbons, Nat. Chem. **6**, 126 (2014).

[28] A. F. Young, C. R. Dean, L. Wang, H. Ren, P. Cadden-Zimansky, K. Watanabe, T. Taniguchi, J. Hone, K. L. Shepard, and P. Kim, Spin and valley quantum Hall ferromagnetism in graphene, Nat. Phys. **8**, 550 (2012).

[29] D. Pesin and A. H. MacDonald, Spintronics and pseudospintronics in graphene and topological insulators, Nat. Mater. **11**, 409 (2012).

[30] X. Zhai and G. Jin, Photoinduced topological phase transition in epitaxial graphene, Phys. Rev. B **89**, 235416 (2014).

[31] M. Sui, G. Chen, L. Ma, W.-Y. Shan, D. Tian, K. Watanabe, T. Taniguchi, X. Jin, W. Yao, D. Xiao, and Y. Zhang, Gate-tunable topological valley transport in bilayer graphene, Nat. Phys. **11**, 1027 (2015).

[32] Q. P. Wu, Z. F. Liu, A. X. Chen, X. B. Xiao, and Z. M. Liu, Full valley and spin polarizations in strained graphene with Rashba spin orbit coupling and magnetic barrier, Sci. Rep. **6**, 21590 (2016).

[33] X. Zhai and G. Jin, Proposal for realizing the quantum spin Hall phase in a gapped graphene bilayer, Phys. Rev. B **93**, 205427 (2016).

[34] P. Vogt, P. De Padova, C. Quaresima, J. Avila, E. Frantzeskakis, M. C. Asensio, A. Resta, B. Ealet, and G. Le Lay, Silicene: Compelling Experimental Evidence for Graphenelike Two-Dimensional Silicon, Phys. Rev. Lett. **108**, 155501 (2012).

[35] L. Tao, E. Cinquanta, D. Chiappe, C. Grazianetti, M. Franciulli, M. Dubey, A. Molle, and D. Akinwande, Silicene field-effect transistors operating at room temperature, Nat. Nanotechnol. **10**, 227 (2015).

[36] C.-C. Liu, W. Feng, and Y. Yao, Quantum Spin Hall Effect in Silicene and Two-Dimensional Germanium, Phys. Rev. Lett. **107**, 076802 (2011).

[37] Z. Ni, Q. Liu, K. Tang, J. Zheng, J. Zhou, R. Qin, Z. Gao, D. Yu, and J. Lu, Tunable bandgap in silicene and germanene, Nano Lett. **12**, 113 (2012).

[38] M. Ezawa, Valley-Polarized Metals and Quantum Anomalous Hall Effect in Silicene, Phys. Rev. Lett. **109**, 055502 (2012).

[39] H. Pan, Z. Li, C.-C. Liu, G. Zhu, Z. Qiao, and Y. Yao, Valley-Polarized Quantum Anomalous Hall Effect in Silicene, Phys. Rev. Lett. **112**, 106802 (2014).

[40] M. Ezawa, Antiferromagnetic Topological Superconductor and Electrically Controllable Majorana Fermions, Phys. Rev. Lett. **114**, 056403 (2015).

[41] W.-F. Tsai, C.-Y. Huang, T.-R. Chang, H. Lin, H.-T. Jeng, and A. Bansil, Gated silicene as a tunable source of nearly 100% spin-polarized electron, Nat. Commun. **4**, 1500 (2013).

[42] A. Yamakage, M. Ezawa, Y. Tanaka, and N. Nagaosa, Charge transport in *pn* and *npn* junctions of silicene, Phys. Rev. B **88**, 085322 (2013).

[43] V. Vargiamidis and P. Vasilopoulos, Polarized spin and valley transport across ferromagnetic silicene junctions, J. Appl. Phys. **117**, 094305 (2015).

[44] T. Yokoyama, Controllable valley and spin transport in ferromagnetic silicene junctions, Phys. Rev. B **87**, 241409(R) (2013).

[45] N. Missault, P. Vasilopoulos, F. M. Peeters, and B. Van Duppen, Spin-and valley-dependent miniband structure and transport in silicene superlattices, Phys. Rev. B **93**, 125425 (2016).

[46] D. Wang, Z. Huang, Y. Zhang, and G. Jin, Spin-valley filter and tunnel magnetoresistance in asymmetrical silicene magnetic tunnel junctions, Phys. Rev. B **93**, 195425 (2016).

[47] X. Zhai and G. Jin, Completely independent electrical control of spin and valley in a silicene field effect transistor, J. Phys.: Condens. Matter **28**, 355002 (2016).

[48] R. Saxena, A. Saha, and S. Rao, Conductance, valley and spin polarizations, and tunneling magnetoresistance in ferromagnetic-normal-ferromagnetic junctions of silicene, Phys. Rev. B **92**, 245412 (2015).

[49] V. P. Gusynin, S. G. Sharapov, and A. A. Varlamov, Anomalous thermospin effect in the low-buckled Dirac materials, Phys. Rev. B **90**, 155107 (2014).

[50] See Supplemental Material at http://link.aps.org/supplemental/10.1103/PhysRevB.94.245405 for the calculated results for (i) single-junction caloritronic device and (ii) robustness of Seebeck effects in our proposed field-effect transistor.

[51] T. Gunst, T. Markussen, K. Stokbro, and M. Brandbyge, First-principles method for electron-phonon coupling and electron mobility: Applications to two-dimensional materials, Phys. Rev. B **93**, 035414 (2016).

[52] P. Wei, S. Lee, F. Lemaitre, L. Pinel, D. Cutaia, W. Cha, F. Katmis, Y. Zhu, D. Heiman, J. Hone, J. S. Moodera, and C.-T. Chen, Strong interfacial exchange field in the graphene/EuS heterostructure, Nat. Mater. **15**, 711 (2016)..

[53] X. Zhai, S. Zhang, Y. Zhao, X. Zhang, and Z. Yang, Bipolar spin-valley diode effect in a silicene magnetic junction, Appl. Phys. Lett. **109**, 122404 (2016).

[54] M. König, A. Tschetschetkin, E. M. Hankiewicz, J. Sinova, V. Hock, V. Daumer, M. Schäfer, C. R. Becker, H. Buhmann, and L. W. Molenkamp, Direct Observation of the Aharonov-Casher Phase, Phys. Rev. Lett. **96**, 076804 (2006).

[55] S. Ghosh and A. Manchon, Signature of topological transition in persistent current in a Dirac ring, arXiv:1607.05052.

[56] J. Schliemann, J. Carlos Egues, and D. Loss, Nonballistic Spin Field-Effect Transistor, Phys. Rev. Lett. **90**, 146801 (2003).

[57] W. Han, R. K. Kawakami, M. Gmitra, and J. Fabian, Graphene spintronics, Nat. Nanotechnol. **9**, 794 (2014).